# Inverse Light Transport (and next Separation of Global and Direct Illumination)

CS434

Daniel G. Aliaga
Department of Computer Science
Purdue University

# Inverse Light Transport

- Light Transport
  - Model transfer of light from "source" (e.g., light/projector) to "destination" (e.g., eye/camera) modulated by scene

light → scene → camera

- Inverse Light Transport
  - Given a photograph of an unknown scene, compute (or decompose) the light into the needed source(s)

light ← scene ← camera

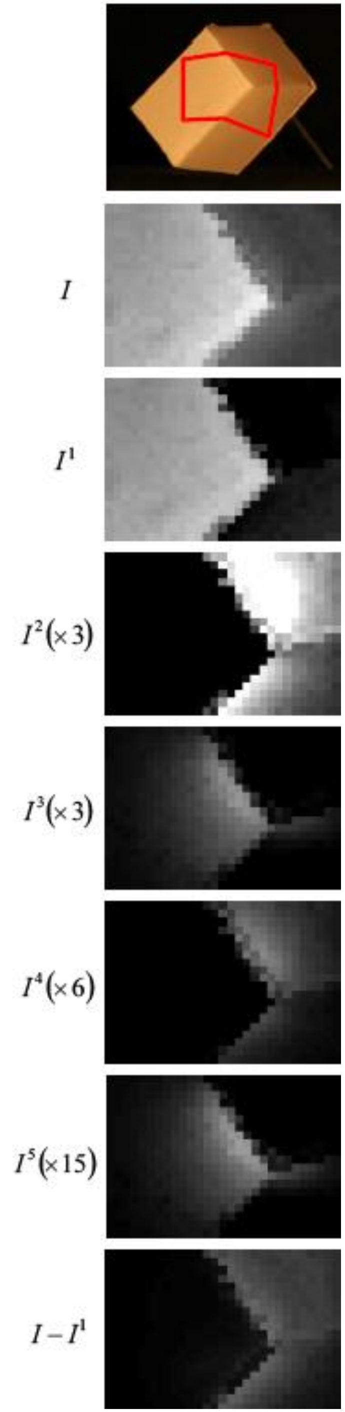
$I$
$I^1$
$I^2(\times 3)$
$I^3(\times 3)$
$I^4(\times 6)$
$I^5(\times 15)$
$I - I^1$

# Topics

- A Theory of Inverse Light Transport
  - Seitz et al., ICCV 2005
- Radiometric Compensation and Inverse Light Transport
  - Wetzstein et al., PG 2007
  - Work at Purdue

# Topics

- A Theory of Inverse Light Transport
  - Seitz et al., ICCV 2005
- Radiometric Compensation and Inverse Light Transport
  - Wetzstein et al., PG 2007
  - Work at Purdue

# Theory of Inverse Light Transport

- Given a photo, decompose it into a sum of **n-bounce images**
- Each bounce image records the light that bounces 'n' times before reaching the camera

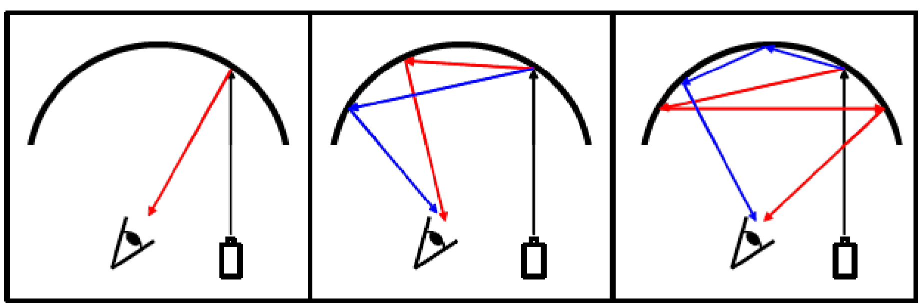

$I^1$ $I^2$ $I^3$

- Formulated for Lambertian scenes

# Theory of Inverse Light Transport

$$I = I^1 + I^2 + I^3 + \ldots + I^n$$

$I^1$ = direct illumination image

$I^i$ = indirect illumination image, for $i \geq 2$

…by removing the $I^i$'s the photographs are converted into a form more amenable to existing graphics/vision processing algorithms

# Formulation

- Outward light field $L_{out}$ from $x$ to point $y$ is

$$L_{out}(x,y) = L_{out}{}^{1}(x,y) + L_{out}{}^{2,3,\ldots}(x,y)$$

- Recall Rendering Equation (or synthetic light-transport equation):

$$I(x,x') = g(x,x')\left[\varepsilon(x,x') + \int_{s} \rho(x,x',x'')I(x',x'')dx''\right]$$

# Formulation

- Outward light field $L_{out}$ from $x$ to point $y$ is

$$L_{out}(x,y) = L_{out}{}^{1}(x,y) + L_{out}{}^{2,3,\dots}(x,y)$$

- Rewrite Rendering Equation as

$$L_{out}(x,y) = L_{out}{}^{1}(x,y) + \int_{x'} A(x',x,y) L_{out}(x',x)\,dx'$$

$A(x',x,y)$ is the proportion of irradiance from $x'$ to $x$ that gets transported to $y$

# Formulation

$$L_{out}(x,y) = L_{out}^{1}(x,y) + \int_{x'} A(x',x,y) L_{out}(x',x)\,dx'$$

$$L_{out}[i] = L_{out}^{1}[i] + \sum_{j} A[i,j] L_{out}[j]$$

for small facets $i,j$

$$L_{out} = L_{out}^{1} + A L_{out}$$

$$L_{out} = ?$$

# Formulation

$$L_{out}(x,y) = L_{out}^{1}(x,y) + \int_{x'} A(x',x,y) L_{out}(x',x)\,dx'$$

$$\Downarrow$$

$$L_{out}[i] = L_{out}^{1}[i] + \sum_{j} A[i,j] L_{out}[j]$$

for small facets $i,j$

$$\Downarrow$$

$$L_{out} = L_{out}^{1} + A L_{out}$$

$$\Downarrow$$

$$\boxed{L_{out} = (I - A)^{-1} L_{out}^{1}}$$

(well-known) maps a light field containing only direct light to a light field having indirect light…

# Cancellation Operator

$$L_{out} = (I - A)^{-1} L_{out}^{\ 1}$$

$$C^1 = I - A$$

$$L_{out} = (C^1)^{-1} L_{out}^{\ 1} \quad \text{or} \quad \boxed{L_{out}^{\ 1} = C^1 L_{out}}$$

which means $C^1$ “cancels the interreflections” in $L_{out}$

# Cancellation Operator

$$L_{out}{}^{1} = C^{1} L_{out}$$

So what is all the light "except for the direct illumination"?

$$L_{out} - C^{1} L_{out}$$

So now the previous "first bounce" indirect light is effectively now the direct illumination component

What is the $L_{out}$ due to the second bounce of light?

$$C^{1}(L_{out} - C^{1} L_{out})$$

# Cancellation Operator

So in general,

$$C^n = C^1(I - C^1)^{n-1}$$
$$L_{out}{}^n = C^n L_{out}$$

where $L_{out}{}^n$ defines the light field due to the $n$-th bounce of light, and

$$L_{out} = \sum_n L_{out}{}^n$$

# Computing $C^1$

For Lambertian scenes, it turns out

$$C^1 = T^1 T^{-1}$$

where $T$ is a light-impulse response matrix similar to that used for dual photography of a diffuse scene (i.e., it is a diagonal matrix)

where $T^1$ is a matrix of the reciprocals of the diagonal elements of $T^{-1}$

# Examples

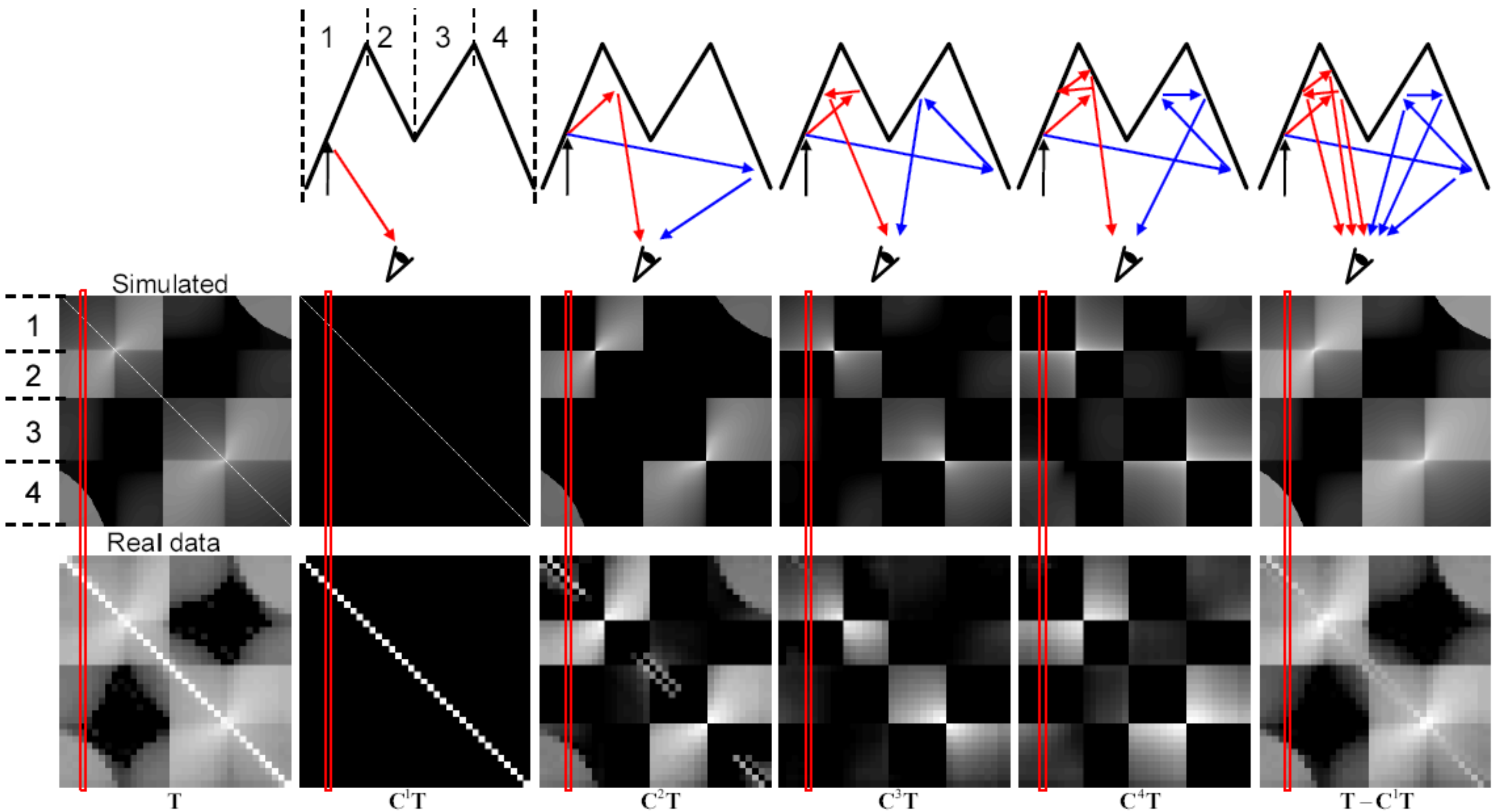


Figure 5: Inverse light transport computed from the ISF matrix **T** for the "M" scene. Top row shows typical light paths, middle row shows simulation results, and bottom row shows results from real-world data. *From left to right:* the ISF matrix, direct illumination (1-bounce), the 2-, 3- and 4-bounce interreflection components of the ISF , and total indirect illumination. Images are log-scaled for display purposes.

# Examples

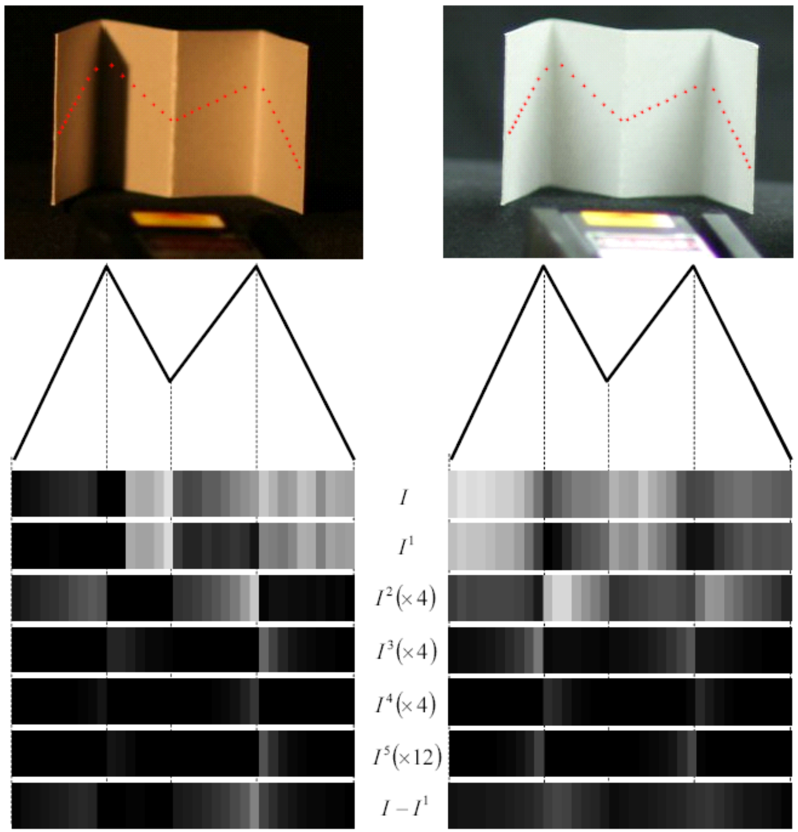


Figure 6: Inverse light transport applied to images $I$ captured under unknown illumination conditions. $I$ is decomposed into direct illumination $I^1$ and subsequent $n$-bounce images $I^n$, as shown. Observe that the interreflections have the effect of increasing brightness in concave (but not convex) junctions of the "M". Image intensities are scaled linearly, as indicated.

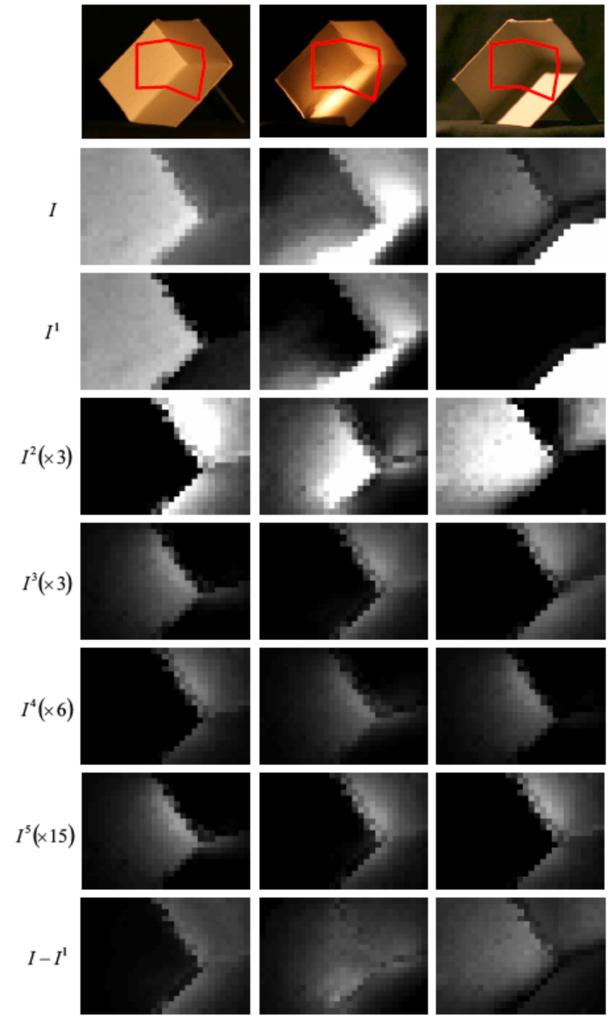


Figure 9: *Inverse light transport applied to images captured under unknown illumination conditions: input images $I$ are decomposed into direct illumination $I^1$, 2- to 5-bounce images $I^2$–$I^5$, and indirect illuminations $I - I^1$.*

# Topics

- A Theory of Inverse Light Transport
  - Seitz et al., ICCV 2005
- Radiometric Compensation and Inverse Light Transport
  - Wetzstein et al., PG 2007
  - Work at Purdue (Aliaga et al. TOG 2012)

# Radiometric Compensation and Inverse Light Transport

- Single projector case (Wetzstein et al. 2007)
  - Theoretically simple, just invert the light transport: $C = TP$

$$P = T^{-1}C$$

$$\left\| P - T^{-1}C \right\| \to 0$$

  - Computation can be expense
    - Bimber spatially decomposes T and uses GPU
    - Success of spatial decomposition is scene dependent

# Example

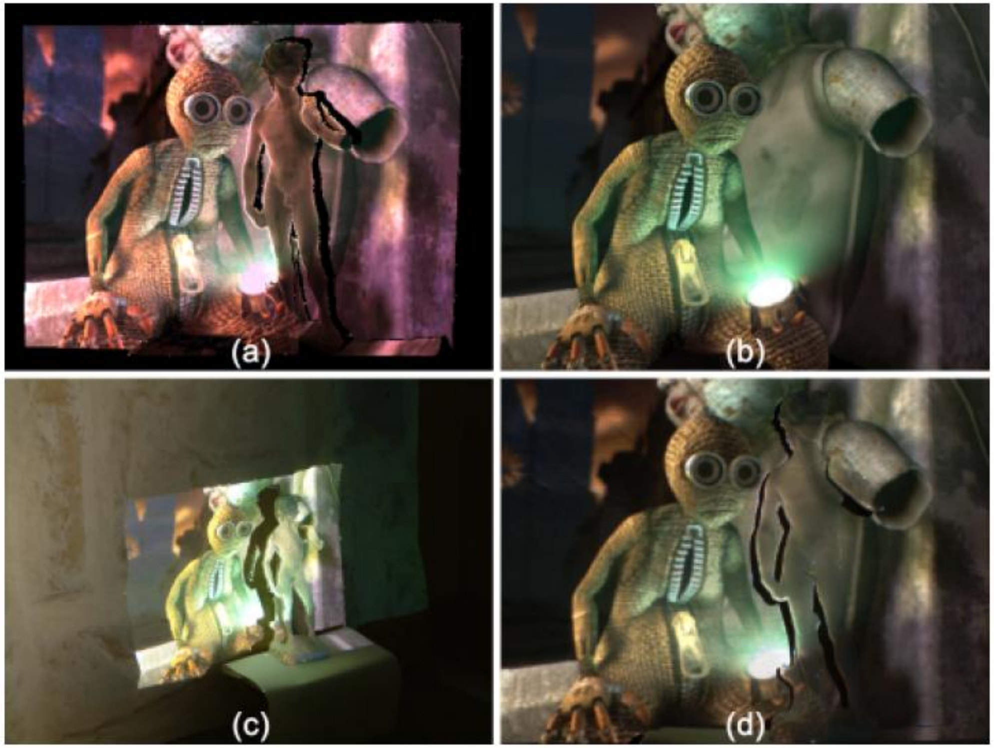


Figure 1. Synthesis of a projector illumination pattern (a) that results in a desired image (b) when projected onto a scene (c) and observed from a predefined viewpoint (d). Note that shadows cannot be removed with a single projector in this example.

# Example

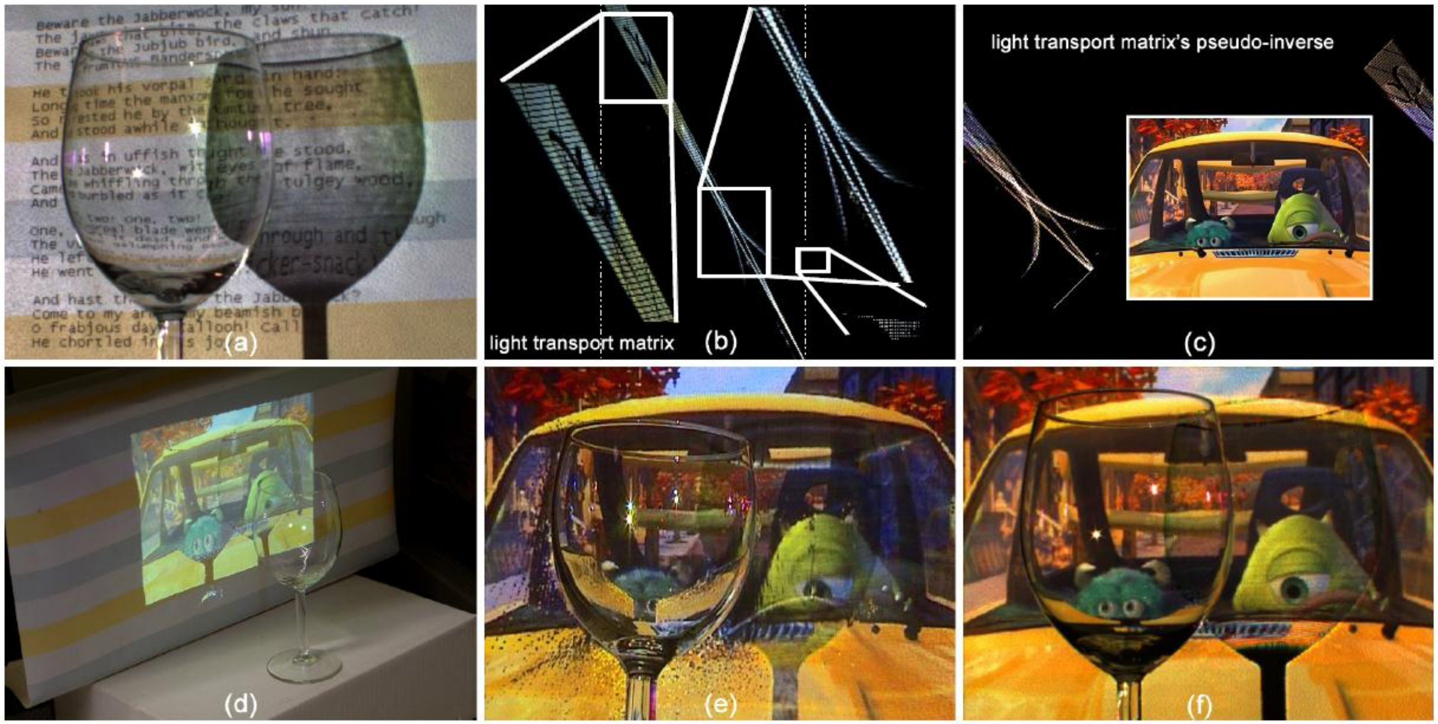


Figure 7. A wine glass in front of a colored wallpaper (a). The light transport matrix's (b) pseudo-inverse (c, background) is approximated with our clustering scheme and allows a real-time compensation for displaying interactive content and movies (c) - from an angle (d), compensated with a conventional method [3] (e) and with our approach (f). Shadows are not removed.

# Radiometric Compensation and Inverse Light Transport

- Multiple projector case
  - More complicated…
  - Need to constrain solution and is computationally much more challenging

# Use ILT to alter appearance

- Alter the appearance of the object's surface

# Single Projector Appearance Editing

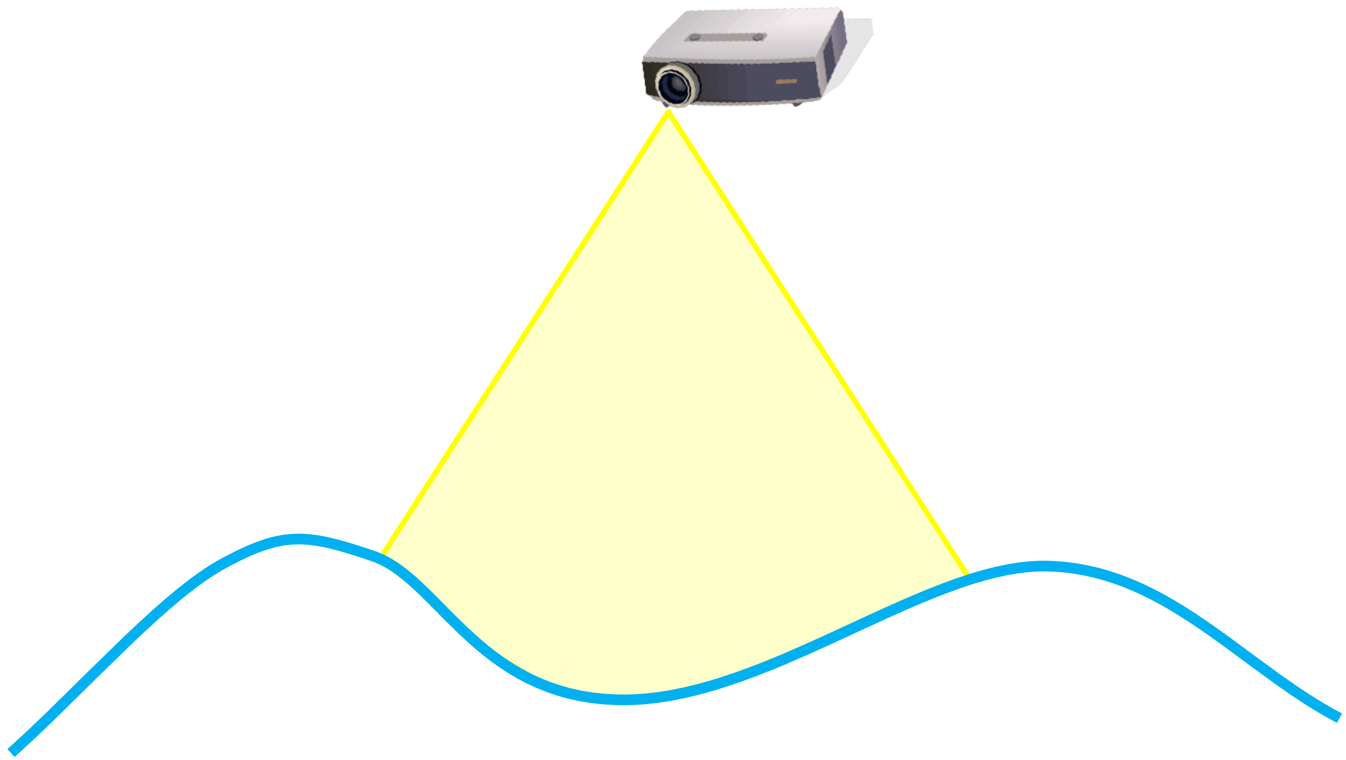

# Multi-Projector Appearance Editing

- Partially overlapping projectors

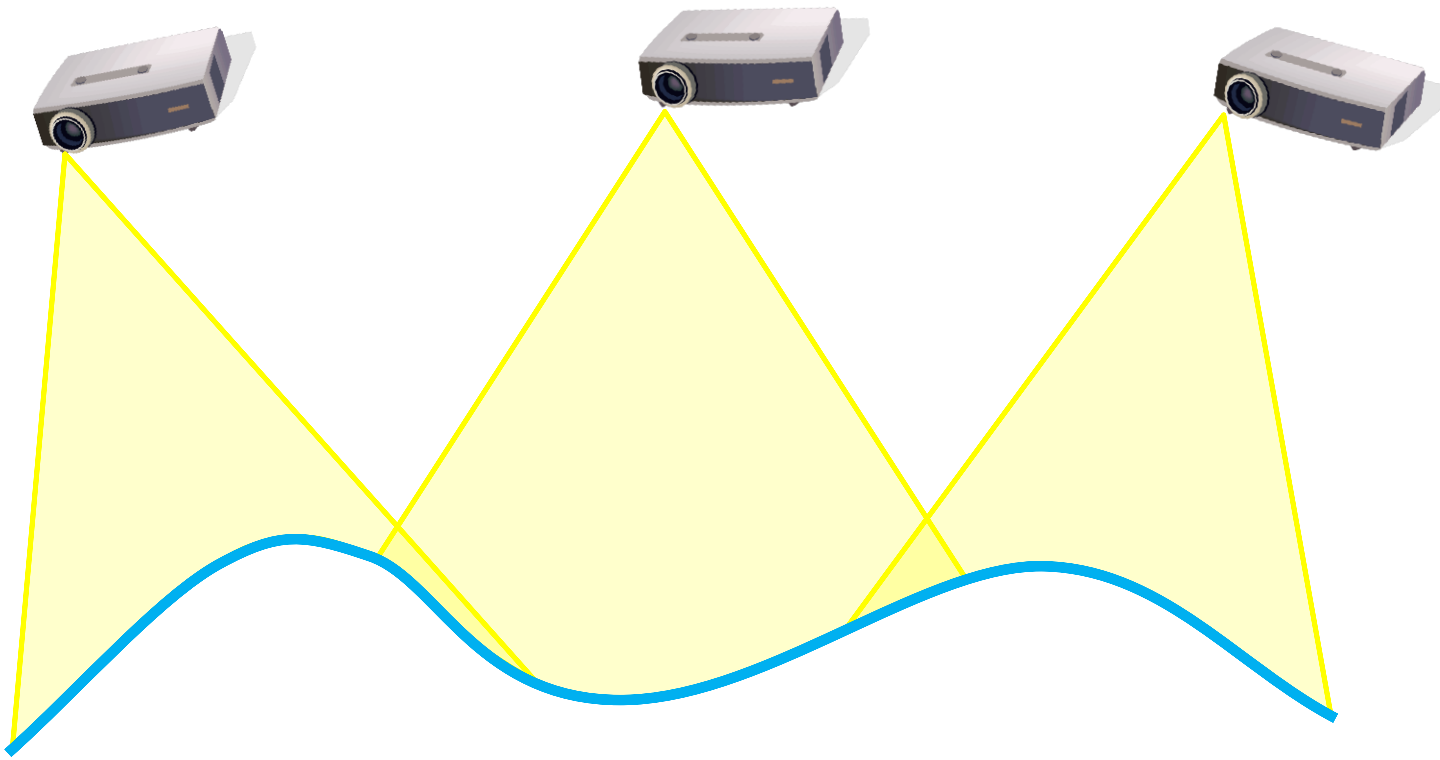

# Multi-Projector Appearance Editing

- Fully superimposed projectors

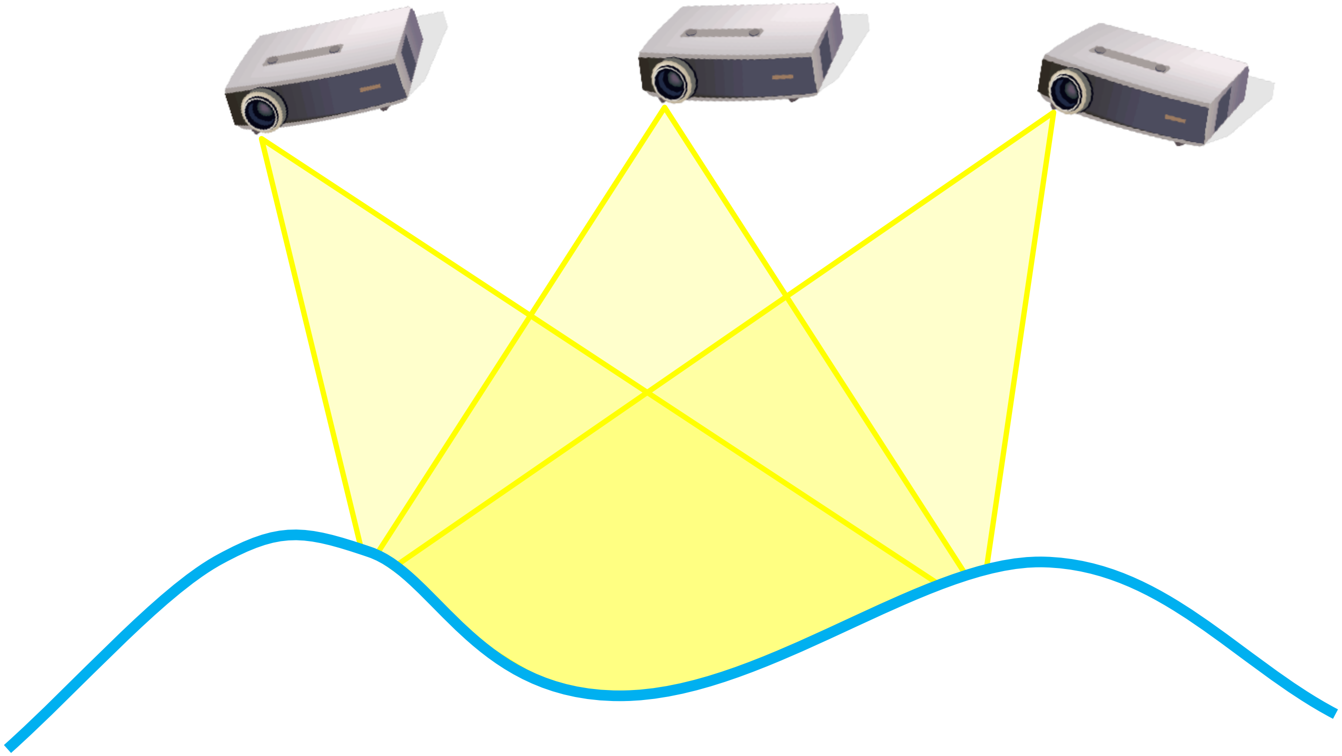

# Multi-Projector Appearance Editing

- Use higher resolution camera to capture projector pixel interaction

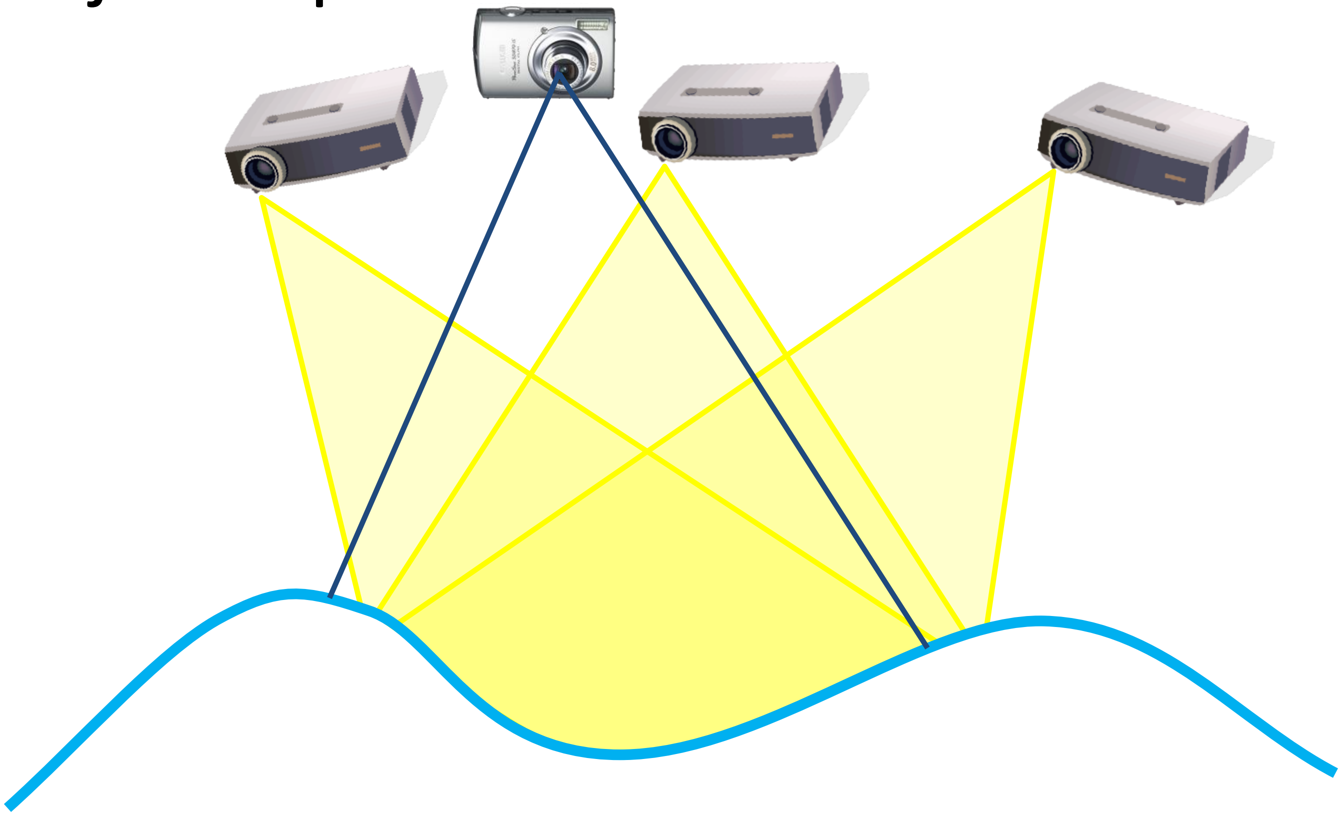

# Overlapping Projector Interaction

# Overlapping Projector Interaction

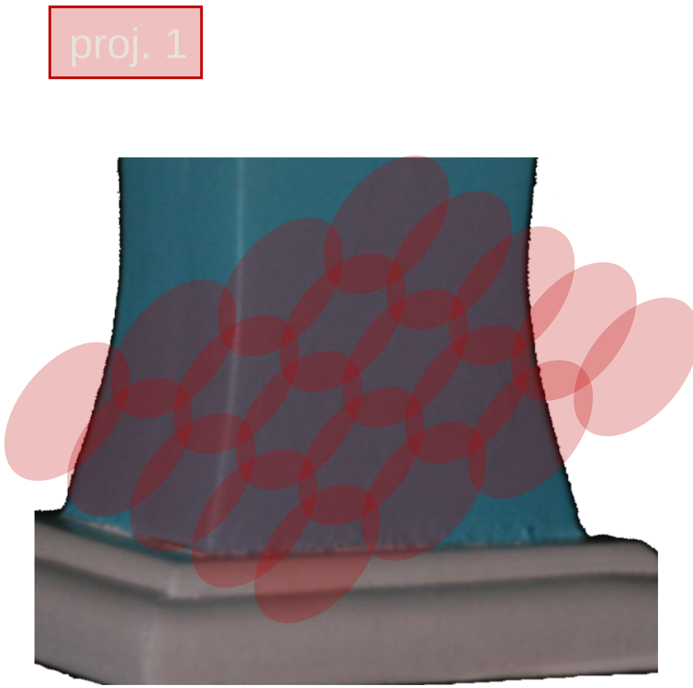

# Overlapping Projector Interaction

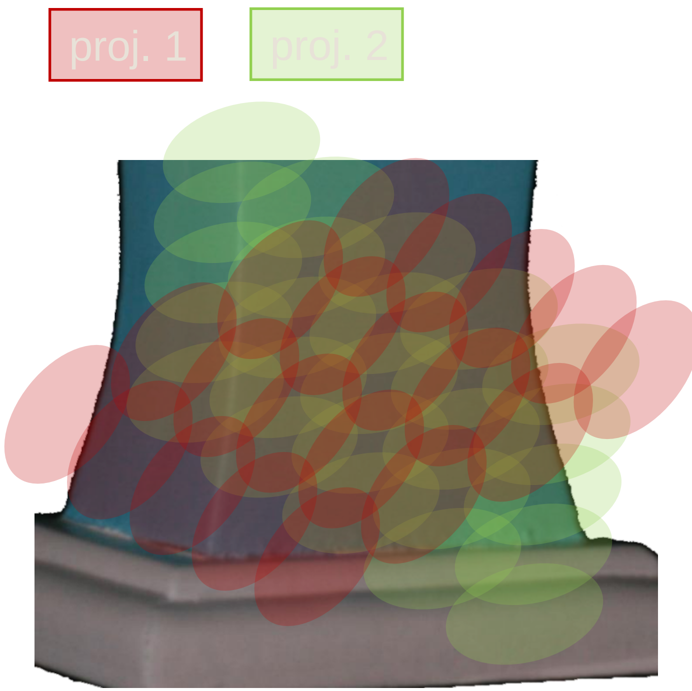

# Overlapping Projector Interaction

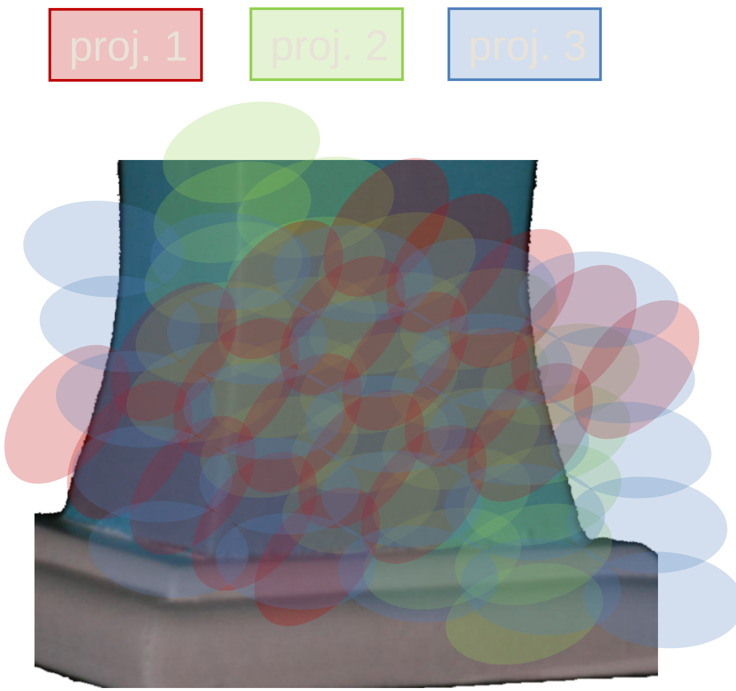

# Overlapping Projector Interaction

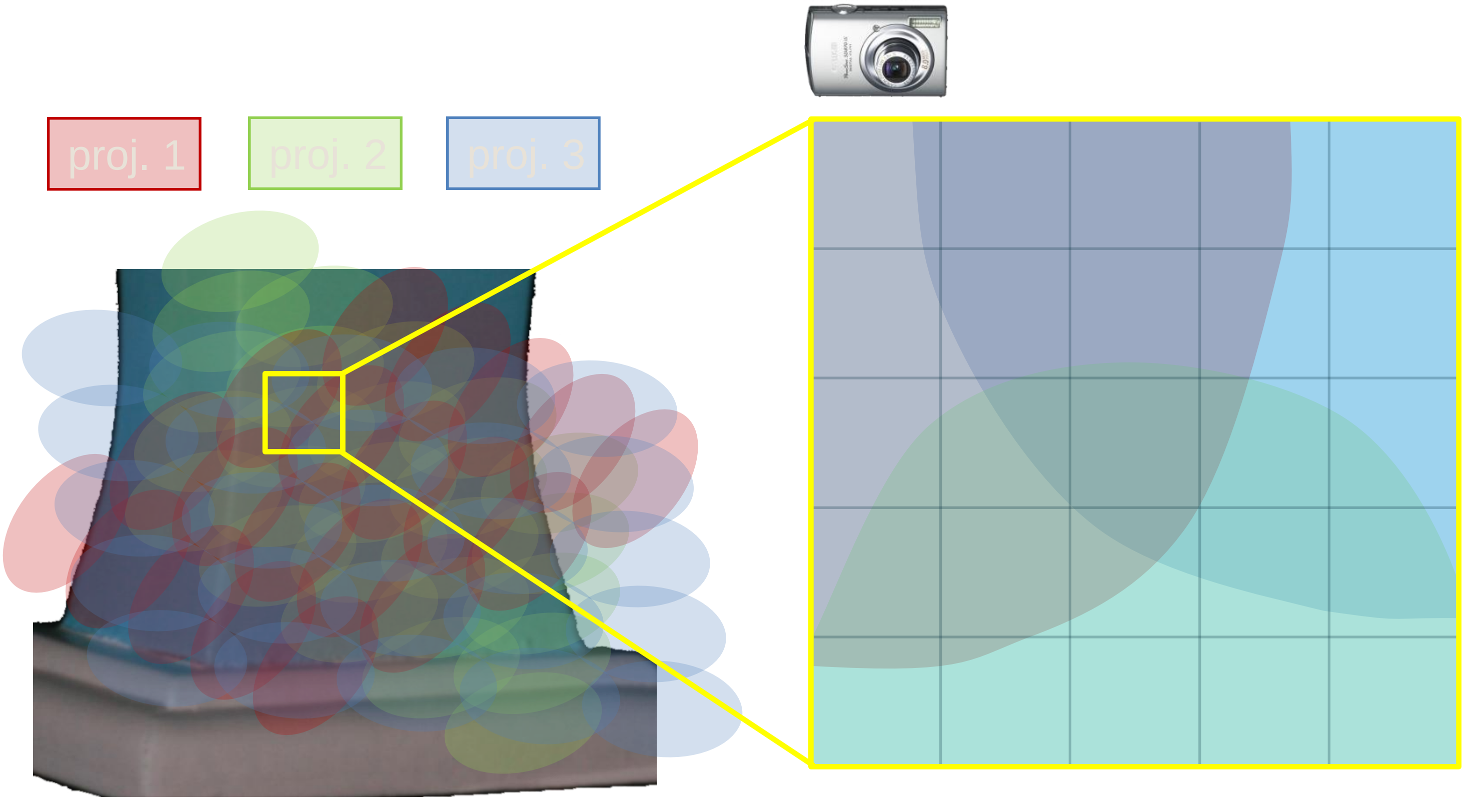

# Overlapping Projector Interaction

- Model metapixels and their interaction within and across projectors

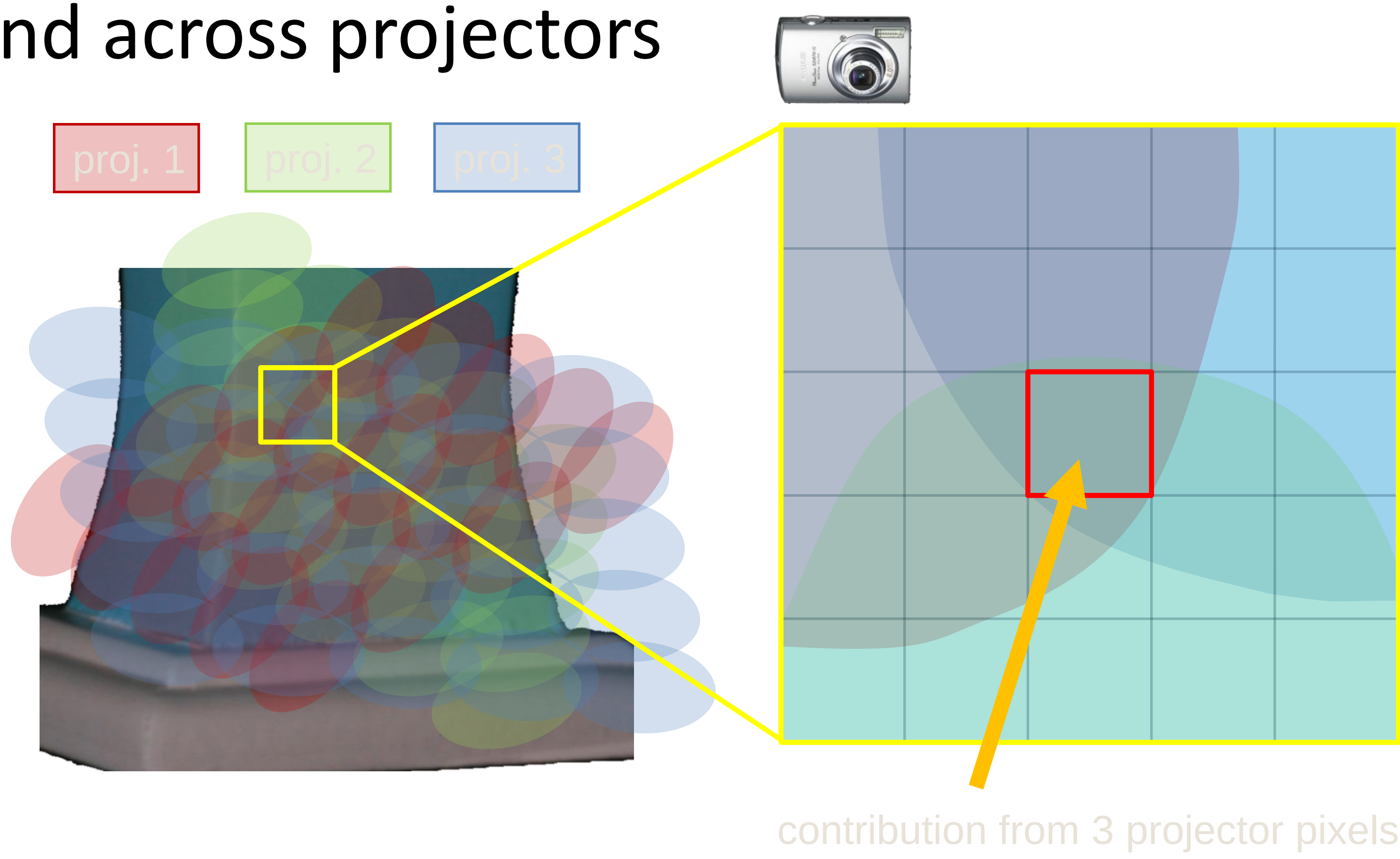

# Challenges

- Efficiently model proj-proj-cam pixel interactions

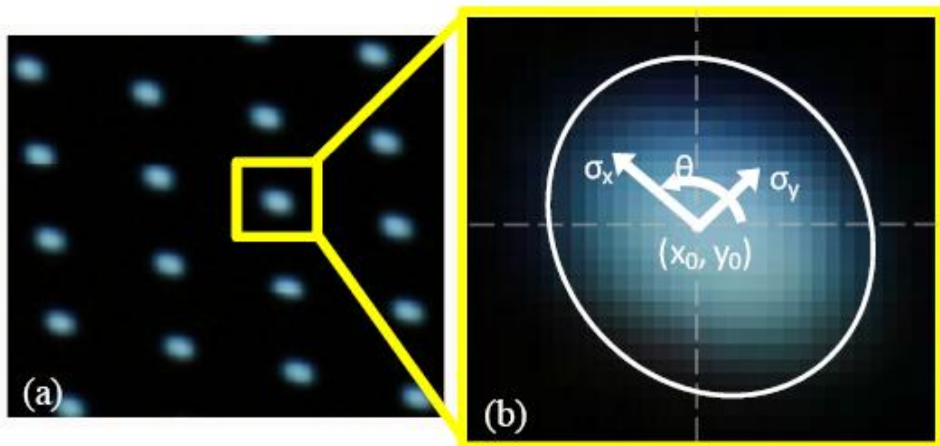


***Figure 6. Projector Pixel Modeling***. *(a) Example metapixels from the acquisition pattern in a camera image used to estimate metapixel parameters. (b) Close-up of a projector pixel on the camera plane and the five metapixel parameters to be refined via a fitting optimization.*

# Challenges

- Constrain solution to produce valid projection values

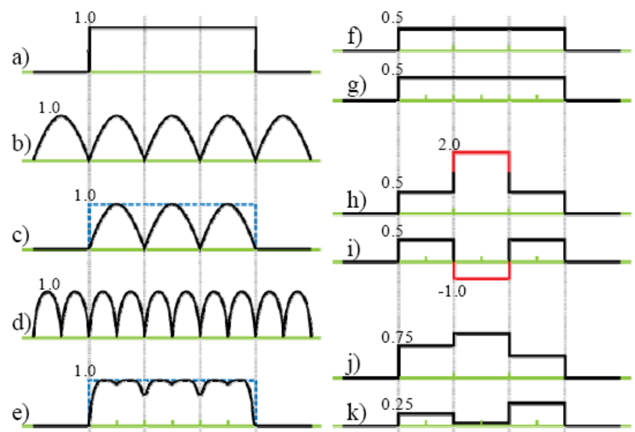


***Figure 3. Multi-Projector Constrained Optimization.*** *(a) Target intensities to achieve across an appearance. (b) Maximum surface illumination intensities from one projector. Each hump represents one projector pixel across the surface. (c) Reconstruction of (a) (dotted) using (b) and appropriate projector intensity values. (d) Maximum surface illumination intensities from a second projector which, in this example, is positioned at a different orientation relative to the object that yields smaller projected pixels. (e) Reconstruction of (a) using both projectors. The reconstruction is more accurate than (c) and more accurate than using only the second projector as well. (f-g) Smooth projector intensities for the two projectors to achieve (e). (h-i) Without illumination constraints, the intensity scales can overflow or underflow as shown in red but theoretically still produce (e). (j-k) Without smoothness constraints, projector intensities may produce noise, shown as intensity undulations.*

# Challenges

- Constrain solution to produce valid projection values

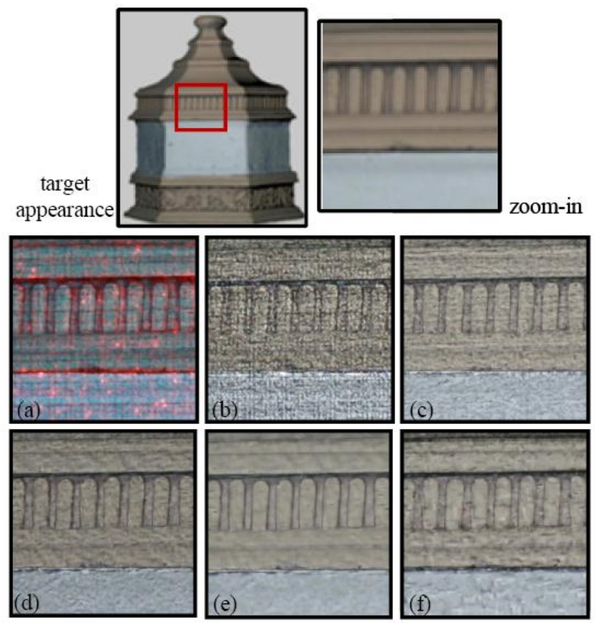


***Figure 8. Comparisons****. Photographs of an appearance-edited house model using the shown target appearance (top row). (a) Naïve inverse light transport optimization computed resulting in artifacts. (b) Constrained optimization to restrict the pixel values to [0,1], but severe noise and graininess still exists. (c) Projector pixel modeling using elliptical Gaussians is added to yield an improved image. (d) Regularization is added to (c) to reduce noise. (e) Smoothness constraints are added to the constrained optimization for a smooth, noise-free appearance. (f) Using quadrilaterals instead of elliptical Gaussians to model projector pixels results in more noise due to inaccurate projector pixel modeling.*

# Examples

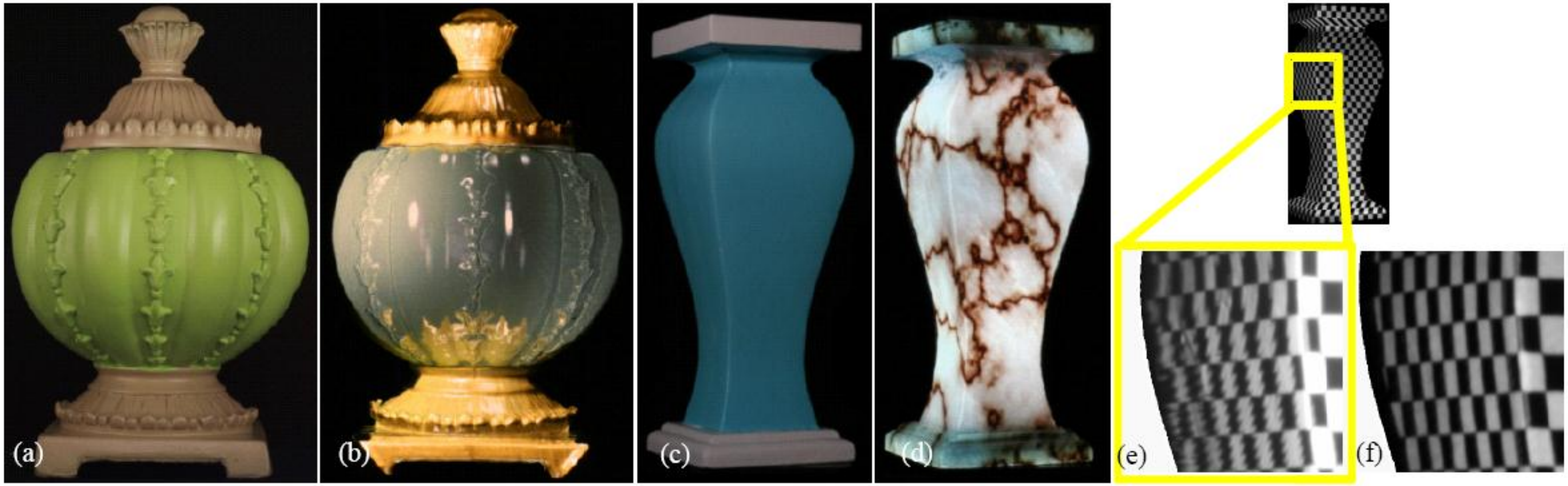


***Figure 1. Fast High-Resolution Appearance Editing.*** *We introduce a framework to model the light interactions between multiple projectors having superimposed fields-of-projection over a surface of arbitrary color and geometry yielding fast and high-resolution appearance editing. All images shown are photographs of objects visible by the naked eye. (a, c) Picture of objects under normal white light. (b) A glossy appearance of the object in (a). (d) A subsurface-scattered marble appearance of (c). A visualization of the resolution improvement achieved by our system: e) one projector, traditional visual compensation and f) results of our multi-projector method.*